UKAEA-CCFE-CP(19)19

C.J. Ham, S.C. Cowley, H.W. Wilson

Nonlinear ballooning flux tubes in tokamak geometry

Nonlinear ballooning flux tubes in tokamak geometry

C.J. Ham, S.C. Cowley, H.W. Wilson

This paper has been submitted to
45th European Physical Society Conference on Plasma Physics (EPS), Prague, 2-6 July 2018

UKAEA-CCFE-CP(19)19

C.J. Ham, S.C. Cowley, H.W. Wilson

Nonlinear ballooning flux tubes in tokamak geometry

Nonlinear ballooning flux tubes in tokamak geometry

C.J. Ham, S.C. Cowley, H.W. Wilson

This paper has been submitted to
45th European Physical Society Conference on Plasma Physics (EPS), Prague, 2-6 July 2018

Nonlinear ballooning flux tubes in tokamak geometry

C.J. Ham[1], S.C. Cowley[2], H.W. Wilson[1,3]

[1] *CCFE, Culham Science Centre, Abingdon, Oxon, OX14 3DB, UK*

[2] *Rudolf Peierls Centre for Theoretical Physics, University of Oxford, Oxford, UK*

[3] *York Plasma Institute, Department of Physics, University of York, Heslington, York UK*

Introduction

Ballooning modes are pressure driven instabilities that occur in the unfavourable curvature region of toroidal magnetic confinement fusion devices [1]. The ballooning instability can lead to either a *soft* or *hard* limit. A soft limit occurs when, say, the pressure profile is held at a critical limit. If the limit is exceeded due to a fluctuation, then the instability is instantly triggered, and the transport caused by the instability brings the profile back to the critical gradient. This process is likely to produce the critical pressure gradient in the pedestal region of H-mode for example. Ballooning modes can also cause hard limits, which are an explosive loss of a significant amount of energy. Hard limits take the profiles very much below the stability limit. Examples of such hard limits are certain types of disruptions [2], possibly the core density collapse in the LHD stellarator [3] and edge localised modes (ELMs) [4]. An improved understanding of what causes these hard limits and how to control them may well improve the economics of fusion energy. We will discuss our theory of nonlinear flux tubes in a general axisymmetric equilibrium and results from a large aspect ratio `s-α' model of a tokamak (where *s* is the magnetic shear and α is the normalized pressure gradient), where we saw metastable flux tubes [5]. We will then show first results using a numerically calculated equilibrium from VMEC. Finally, we will give our conclusions.

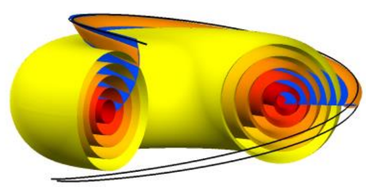

Figure 1: Elliptical (orange) flux tube sliding along (blue) surface S parting surrounding (black) field lines. The tube's displacement is larger on the outboard side of the flux surfaces – the tube balloons. The magnetic shear ($s = rq'/q$) causes the twist and narrowing of the tube on the inside.

Flux tubes in a general axisymmetric equilibrium

We consider the dynamics of an isolated flux tube with an ideal MHD model. The derivation here follows Ham *et al.* [5]. We will assume that the flux tube moves more slowly than the sound speed, because we are interested in the saturated states near marginal stability. We assume that there is a magnetic field inside the flux tube $\mathbf{B}_{in}$ and the ambient field outside which we will denote $\mathbf{B}_{out}$. The flux tube is field aligned. The flux tube is restricted to move on a surface that is parallel to the ambient magnetic field lines at each location. This surface twists with radius as the magnetic field is sheared, see figure 1. We call this surface S and note that we can write the magnetic field using S as a Clebsch potential

$$B = \nabla\psi \times \nabla S \quad \text{with} \quad S = \phi - q(r)(\theta - \theta_0) \qquad (1)$$

The flux tube is assumed to have an elliptic cross section. This shape minimises the field line bending of the ambient magnetic field but it is also indicated by the weak nonlinear theory [7]. We emphasize that the flux tube shape does not come out of the theory presented here; it is a justified assumption. The flux tube will be assumed to have dimensions δ_1 and δ_2 where $\delta_2 >> \delta_1$, see figure 2.

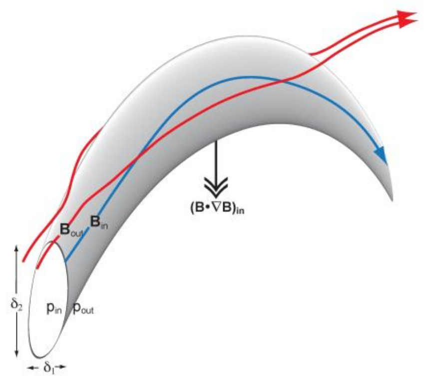

Figure 2: The flux tube is elliptical in shape with δ_1, in the binormal direction, much smaller that δ_2, in the radial direction.

The flux tube will be assumed to have a trajectory $r(\theta,r_0,t)$ on a surface, S=constant. The displacement decays along the field line to the original flux surface i.e. $r(|\theta|\rightarrow\infty ,r_0,t) \rightarrow r0$ where θ measures the distance along the field line.

We use the ideal MHD force, $F = J \times B - \nabla p$, to calculate the forces on the flux tube,

$$F = -\frac{1}{\mu_0}\nabla\left[\frac{B^2}{2} + \mu_0 p\right] + \frac{1}{\mu_0} B \cdot \nabla B \qquad (2)$$

We resolve the forces in the ∇S direction and in the direction along S (the force is formally large in the ∇S direction and must cancel) which gives the following formulae

$$\mu_0 p_{in} + \frac{B_{in}^2}{2} = \mu_0 p_{out} + \frac{B_{out}^2}{2} \quad \text{and} \quad F_\perp = \frac{1}{\mu_0}[B_{in} \cdot \nabla B_{in} - B_0 \cdot \nabla B_0] \cdot e_\perp \qquad (3a, b)$$

where $e_\perp = \frac{1}{B_0}\nabla S \times B_0$. The perpendicular force is calculated from equations (3). The rest is geometry. If we linearize this equation we get the ballooning equation of Connor [1].

Nonlinear flux tubes in large aspect ratio toroidal geometry

We have evaluated the perpendicular force equation for the `s-α' large aspect ratio toroidal expansion in recent publications [5,6]. The key result from this work is that there are flux tubes that are linearly stable, and in fact the whole equilibrium can be linearly stable, yet there are flux tubes that have energetically favourable saturated states that have finite ballooned displacements. These displacements can be as large as the transport barrier width within the `s-α' model. Investigations from the `s-α' model showed that flux tubes could be categorised into one of four states. The flux tube can be stable and have no saturated states available. Alternatively, it can be linearly stable but have either a higher or lower energy displaced state available. Finally, the flux tube can be unstable and have two displaced states available (one moving in and one out).

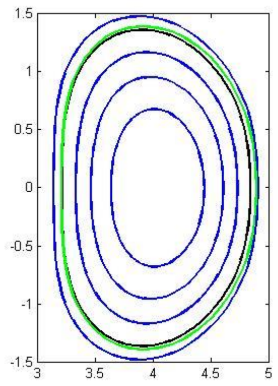

Figure 3: Tokamak geometry showing the saturated fluxtube, in green. The blue line denote the flux surfaces in the plasma

Nonlinear flux tubes in realistic toroidal geometry

We can also evaluate the required geometry from a numerical equilibrium, we use VMEC here [8]. This allows us to calculate the states in realistic geometry. The equilibrium from VMEC is translated to Boozer coordinates. We can then derive the elements of the metric tensor which allows us to calculate the required quantities for the nonlinear ballooning equation. We have successfully tested the results from our numerical calculation against the `s-α' model. These first results are restricted to up-down symmetric cases for computational convenience, this will be relaxed in future work.

The flux tube saturated states are calculated here by assuming a viscous drag will act in opposition to the MHD perpendicular force. This allows the saturated flux tubes to be found by allowing the system to saturate. The flux tube is given an initial perturbation and the simulations run until the flux tubes reach a saturated state. We can demonstrate the calculation in a realistic tokamak geometry by looking at an aspect ratio 4 shaped cross section tokamak, cross section and displaced flux tube shown in figure 3. Figure 4 shows the evolution of a perturbed flux tube to its saturated state for the equilibrium shown in figure 3. This case is for an unstable flux tube. The results from the numerical equilibrium are in qualitative agreement with the 's-α' model. In particular the `s-α' geometry showed that the metastable fluxtubes were more likely to occur at low shear. We have calculated a VMEC equilibrium which has linearly stable flux tubes but these flux tubes also have nonlinearly saturated states. This shows that metastability is not just an artefact of the `s-α' geometry but that we must expect to see it in real tokamak plasmas.

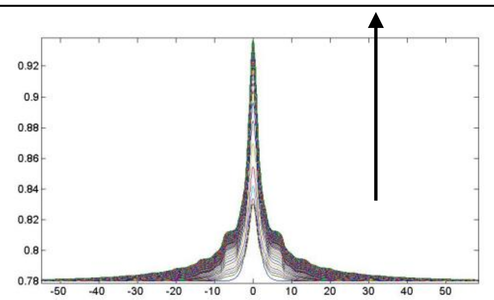

Figure 4: The evolution of a flux tube with time under viscous drag. Horizontal axis is distance along the field line. Vertical axis is the minor radius. The displacement is localized around the outboard midplane. The unstable flux displacement saturates.

The evolution of the flux tube to a displaced saturated state is unlikely to be the end point of the evolution of the flux tube. We would expect that other - non-ideal – processes will occur. There will be an angle between the magnetic field inside the flux tube and the ambient field around it. This will produce a current sheet around the flux tube and the magnitude of this current sheet will be proportional to the angle between the field lines. We may well expect magnetic reconnection to occur where this current sheet is at its greatest. We can calculate the angle using $\cos(\theta) = (B_{in} \cdot B_{out})/(|B_{in}||B_{out}|)$. The angle at which this is greatest is around 75° for the flux tube in figure 4. This angle may well reduce for higher magnetic shear or increased shaping.

Conclusions and future work

We have demonstrated that we can calculate nonlinear ballooning filaments, not only in a large aspect ratio analytic geometry, but also in realistic up-down symmetric tokamak geometry. (We expect to find them in up-down asymmetric plasmas in future work.) We have also shown that we can find metastable flux tubes in these realistic geometries. This gives us cause to believe that these states will exist in tokamak plasmas. We will examine equilibria reconstructed from experimental data in future work. The region of low magnetic shear, due to the bootstrap current, and high-pressure gradient, which we see in the pedestal region of H-mode tokamak plasmas, must be an important area for future investigation.

We have discussed the possible magnetic reconnection due to the current sheet that would surround the flux tube however other non-ideal processes may occur and we will investigate these in future work.

CJH would like to thank Guillermo Bustos Ramirez, Jarrod Leddy, Samuli Saarelma, Costanza Maggi, Fulvio Militello, Stanislas Pamela and the members of the EUROfusion 'Filament reconnection' enabling research grant for their help and useful discussions. We would also like to thank S P Hirshman for the use of VMEC. This work has been carried out within the framework of the EUROfusion Consortium and has received funding from the Euratom research and training programme 2014-2018 under grant agreement No 633053 and from the RCUK Energy Programme [grant number EP/P012450/1]. To obtain further information on the data and models underlying this paper please contact PublicationsManager@ukaea.uk. The views and opinions expressed herein do not necessarily reflect those of the European Commission.

[1] J W Connor, R J Hastie and J B Taylor, *Proc. R. Soc. London* **A365** (1979) 1-17

[2] E D Fredrickson *et al* Phys. Plasmas **3** (1996) 2620

[3] S Ohdachi *et al* Nuclear Fusion **57** (2017) 066042

[4] M. Willensdorfer et al 'Dynamics of ideal modes and subsequent ELM-crashes in 3D tokamak geometry from external magnetic perturbations' submitted to *Plasma Phys. Control Fusion*

[5] C J Ham *et al* Plasma Phys. Control Fusion **60** (2018) 075017

[6] C J Ham *et al* Phys Rev. Lett. **116** (2016) 235001

[7] H R Wilson and S C Cowley Phys Rev. Lett. **92** (2004) 175006

[8] S P Hirshman and J C Whitson Phys Fluids **26** (1983) 3553